Journal of Mining and Earth Sciences

Analyzing of land subsidence by Sentinel-1 time-series images using PSInSAR method: A case study of Thai Nguyen, Vietnam

Hang Minh Le [1,*], Anh Van Tran [2]

[1] *Le Quy Don Technical University, Hanoi, Vietnam*
[2] *Hanoi University of Mining and Geology, Hanoi, Vietnam*

ARTICLE INFO	ABSTRACT
	Natural disasters and human activities are now causing an increase in land subsidence, or surface displacement. The effects of land subsidence cause landslides and construction cracking. PSInSAR (Persistent Scatter Interferometry) was identified to estimate surface displacement from a time series of Synthetic Aperture Radar (SAR) images. This technique is a subset of the DInSAR (Differential Interferometric Synthetic Aperture Radar) method. In this article, the authors determined and analyzed land subsidence in Thai Nguyen Province, Vietnam, using time series Sentinel-1A data with VV polarization from July 2019 to December 2020 and the PSInSAR method. There are numerous mineral exploitation mines in Thai Nguyen Province. It is one of the causes of an unusual amount of land subsidence in the region. According to the results determined by the InSAR technique, the velocity of displacement along the line of sight (LOS) of the study area ranges from -23.2 mm per year to +21.0 mm per year. The analysis of time-series SAR images reveals anomalous land subsidence at persistent scatter (PS) points. By analyzing the time-series displacement at PS points using the StaMPS Visualizer tool, the land subsidence during the image acquisition period and surface displacement trends over time were determined. According to this, coal mining regions have the highest land subsidence values ranging from -40 mm to -60 mm. The city and mine regions of Thai Nguyen, where operations have stopped, are largely stable. In addition, the time-series analysis at PS points will allow us to identify unusual displacement points, enabling the implementation of early warning plans.

1. Introduction

Land subsidence occurs more frequently due to climate change and human activities such as agriculture, mining, industry development, or groundwater extraction (Conacher and Conacher, 1995). Subsidence is one of the types of vertical

displacement and the most common form of surface deformation. Land subsidence is uneven at each locality, leading to slides on a larger regional scale, causing severe damage. The traditional method for land subsidence detection is leveling surveys. This method produces high-quality data, but it is time-consuming, costly, labor-intensive, and difficult to monitor a large area. Hence, InSAR was applied to determine terrain altitude with extensive spatial coverage, fine resolution, and high accuracy.

Many studies proposed determining land subsidence by using the DInSAR method. DInSAR interferometry can extract the phase difference between different radar images by combining them with a digital elevation model (DEM), which allows for centimeter-level accuracy in measuring surface displacement (Bateson et al., 2015). In contrast, the accuracy of the DInSAR method depends on the perpendicular baseline, the atmospheric changes, and the phase noise (Pepe and Calo, 2017). The wavelength of radar has an effect on the phase noise of SAR interferograms. The different wavelengths of radar are used to determine land subsidence by using the DInSAR method, including ERS 1, 2 (Bateson et al., 2015), RadarSAT (Zhang et al., 2019), TerraSAR-X (Tran et al., 2021a), and ALOS PALSAR images (Dang et al., 2014). Long-wavelength radar systems, such as ALOS PALSAR, have been shown to be less accurate than ERS radar systems in measuring LOS displacement via SAR interferometry (Sandwell et al., 2008). Besides, the Atmospheric Phase Screen (APS) is one of the primary sources of error in SAR interferometry and depends on the heterogeneity of the atmosphere, which includes variations in local temperature, pressure, and humidity. The delay of the signal affects the phase error in the interference (Emardson et al., 2003). In particular, topographic changes have a high correlation with APS (Delacourt et al., 1998). Therefore, in order to limit atmospheric effects, APS needs to be determined and compensated in a series of interferences by finding phases that are highly correlated with topography (Balbarani et al., 2013). Time series InSAR data are processed to determine land subsidence, such as through the analysis of multi-temporal DInSAR data, the PSInSAR method (Chen et al., 2018b; Ferretti et al., 2001), the Small BAseline Subset Interferometry (SBAS) method (Bateson et al., 2015; Chen et al., 2018a), and combination with PSInSAR and SBASInSAR (He et al., 2020). PSInSAR and SBASInSAR methods have improved accuracy and reduced the atmospheric effects of the DInSAR method.

The European space agency (ESA) successfully launched the Sentinel-1 satellite in April 2014, and now it has Sentinel-1A and Sentinel-1B satellites. However, on August 3, 2022, the ESA announced that the Sentinel-1B satellite would be decommissioned following many repair attempts. The Sentinel-1 satellite carries a microwave sensor with band C, a 12-day cycle, high spatial resolution, a 250-kilometer with wide swath, and no charge. Sentinel-1 image is a dual-polarization image including VV and VH. Much research proposed to use Sentinel-1 time series images and DInSAR techniques to determine land subsidence on the Earth (Deng et al., 2019).

In Vietnam, Tran et al. (2007) used JERS-1 data and the DInSAR method to estimate land subsidence in the Hanoi area from 1995 to 1998, with a rate of -3.3 cm/year. Besides, time-series TerraSAR-X (Tran et al., 2021a) and COSMO-SkyMed data (Tran et al., 2021a; Tran et al., 2016) were used and processed by the PSInSAR methodology to determine land subsidence in the Hanoi urban area from 2011 to 2014. Sentinel-1 data were used to determine land subsidence in mining areas by using PSInSAR (Nam, B. X. et al., 2021; Tran et al., 2020; Tran et al., 2021b). Sentinel-1 data enables accurate surface displacement detection in barren land areas without plant cover or urban areas. The permanent scattering points and the surveying points using GNSS have a high correlation value of more than 0.83.

In this study, we propose to analyze land subsidence using the PSInSAR method and Sentinel-1A time-series data.

2. Study area and materials

2.1. Study area

The study area is conducted at Trai Cau Iron Mine and Thai Nguyen City in the Thai Nguyen province, Vietnam (Figure 1a). The Trai Cau iron mine, which is a huge iron mine in the Dong Hy
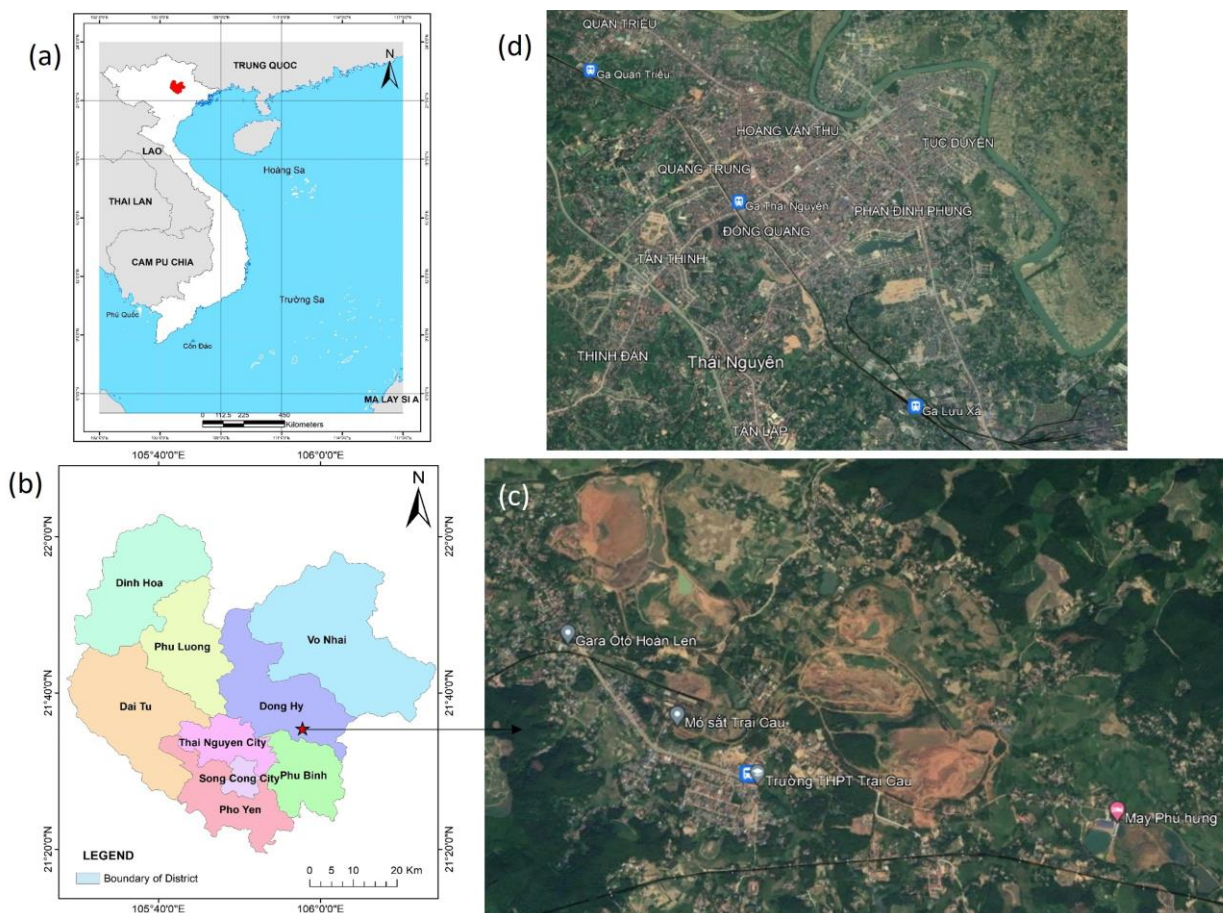
Figure 1. (a) Location of the study area in Vietnam; (b) Location of the districts in Thai Nguyen province; (c) Trai Cau iron mine of Dong Hy district; (d) Thai Nguyen city.

district of Thai Nguyen province, was built in 1959. However, some residents' houses in Dong Hy district were reported to have cracked in 2016 and 2017. According to research results, the Trai Cau Mine's activities have an impact on the subsidence of the surrounding area (Dan, 2018). To evaluate the subsidence of the study area, we propose to use time series Sentinel-1 images, which were taken in Trai Cau Iron Mine and Thai Nguyen City.

The study area is in the midland. The weather is quite hot and humid. Summer brings a lot of rain. The yearly rainfall averages between 1,500 and 2,000 mm. There are the Cau River System and the Linh Nham River (a tributary of the Cau River). From May through October, the rainy season is the flood season. Thai Nguyen province frequently experiences major subsidence because of the difference in topography and heavy rainfall in the summer.

2.2. Materials

The parameters of data are shown in Table 1. The position of the study area is the subswath IW2 of Sentinel-1A. The data is processed by SNAP toolbox software. In this article, 44 Sentinel-1A images were used. Table 2 shows the length of the perpendicular baseline and Figure 2 illustrates

Table 1. The characteristics of the materials.

The parameters	Sentinel-1 data
Satellite	Sentinel-1A
Swath mode	IW (Interferometric Wide)/ IW2
Level	SLC (Single-look Complex)
Polarization	VV

Table 2. Information of image acquisition dates and the length of the perpendicular baseline.

No	Date	Perpendicular baseline (m)	No	Date	Perpendicular baseline (m)
1	04/03/2020	0	23	28/03/2020	-22.66
2	08/07/2019	24.26	24	09/04/2020	-14.22
3	20/7/2019	-17.72	25	21/04/2020	-23.62
4	01/08/2019	87.53	26	03/05/2020	-11.47
5	13/08/2019	-59.82	27	15/05/2020	-0.21
6	25/08/2019	-80.53	28	27/05/2020	-8.20
7	06/09/2019	-71.11	29	08/06/2020	60.81
8	18/09/2019	15.80	30	20/06/2020	-22.04
9	30/09/2019	-54.22	31	14/07/2020	28.04
10	12/10/2019	69.33	32	26/07/2020	-66.72
11	24/10/2019	88.19	33	07/08/2020	12.16
12	05/11/2019	-42.66	34	19/08/2020	72.36
13	17/11/2019	-68.02	35	31/08/2020	-23.57
14	29/11/2019	8.62	36	12/09/2020	-87.29
15	11/12/2019	64.09	37	24/09/2020	-94.90
16	23/12/2019	57.84	38	06/10/2020	-69.85
17	04/01/2020	33.01	39	18/10/2020	29.17
18	16/01/2020	10.19	40	11/11/2020	28.63
19	28/01/2020	-4.38	41	23/11/2020	18.74
20	09/02/2020	16.86	42	05/12/2020	-15.89
21	21/02/2020	24.30	43	17/12/2020	-26.73
22	16/03/2020	-49.64	44	29/12/2020	53.38
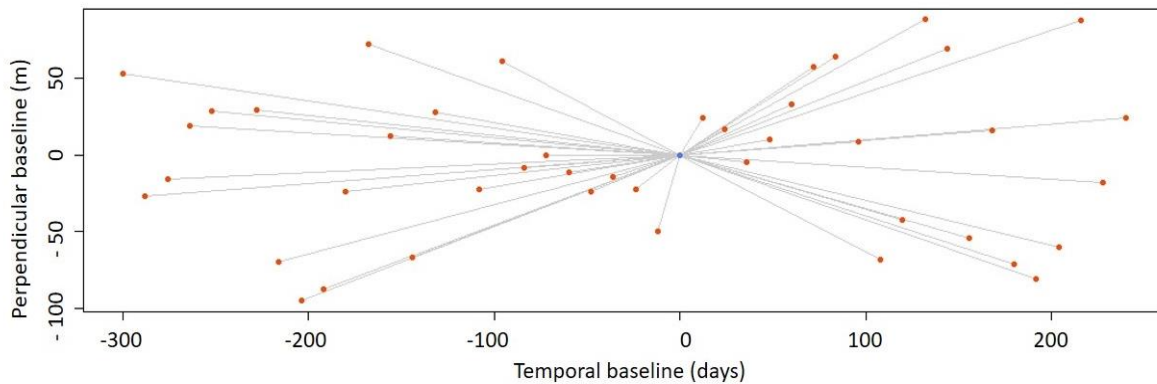
Figure 2. The temporal baseline plot of experience data.

the baseline distribution over time. The master image was chosen on March 04th, 2020 and the others were the slave images.

3. Methodology

3.1. DInSAR method (Differential Interferometric Synthetic Aperture Radar)

Interferometric Synthetic Aperture Radar, is a radar technology used to measure surface deformations over time in the same area. This approach makes use of two or more SAR images to accurately create a surface displacement map over days or years or calculate DEM. If digital elevation model data is available, the terrain displacement may be calculated by subtracting the ground points' altitude from the

interferometric phase (so-called differential interferogram) (Ferretti et al. 2007). DInSAR is used to identify earthquakes, landslides, and subsidence at the slightest relative positional changes of ground points between two SAR images. The following is the determination of the interferogram phase or possible displacement of the scatterer on the ground between observations:

$$\Delta\phi_d = \frac{4\pi}{\lambda} \cdot r \qquad (1)$$

In which: λ - the wavelength of radar; d - the relative scatter displacement projected on the slant range direction.

However, while determining the components related to displacement by the DInSAR technique, some components contain errors such as the accuracy of terrain and orbital parameters. In addition, there are some effects on phase accuracy, such as the change in the atmospheric and ionospheric dielectric constant between the two master/slave acquisitions and phase noise (Pepe and Calo, 2017).

3.2. PSInSAR method (Persistent Scatterer Interferometry Synthetic Aperture Radar)

One of the innovative methods of DInSAR approaches is the PSInSAR method. By detecting permanent scatterers in the series of InSAR data, the PSInSAR technique reduces the effect of the atmosphere and signal noise of the DInSAR method.

Figure 3 illustrates the PSInSAR method. In PSInSAR method, one image as the master is chosen and the others as slave images are co-registered together with the master image.

In Figure 3, the point P is identified by N times in different scanning tracks. The interferogram is calculated by two complex images in Eq.(2) (Bamler and Hartl, 1998).

$$\varphi_{t1,t2} = \varphi_{t1} - \varphi_{t2}$$
$$= \left(\frac{4\pi}{\lambda}R_{t1}(P) + \alpha(t1)\right)$$
$$- \left(\frac{4\pi}{\lambda}R_{t2}(P) + \alpha(t2)\right) \qquad (2)$$

In which: φ_{t1} - the interferometric phase for the *t1* acquisition; φ_{t2} - the interferometric phase for the *t2* acquisition; $R_{t1}(P)$ and $R_{t2}(P)$ - the slant ranges from the *t1* and *t2* antennas to the P point on the Earth surface, and $\alpha(t1)$ and $\alpha(t2)$ - the phase errors of atmosphere propagation of the two times.

Eq. (3) can be written as follows if there is terrain displacement:

$$R_n(P) = R_{n0} + v(P).t_n \qquad (3)$$

In which: $v(P)$ - indicates the Linear Deformation Rate and t_n - the time taken to acquire the n pass.

Ferretti and et al. (2007) showed that the information of the topographic phase and the displacement phase between the two acquisitions of the target were recorded in the interferometric phases. We assume that each pixel in the SAR image is a target to be identified by the total of many scattering responses. As a consequence, a stochastic process is realized, with the pdf conditioned on the interferometric phases considered as a zero-mean, multivariate circular normal distribution (Bamler and Hartl, 1998). Hence, the ensemble of the second order moment provides enough statistics to derive information from image data. Eq. (4) is the expression of the second-order moment for the *t1t2* interferometric pair with reference to a specific position in the slant range–azimuth plane, as follows:

$$E[y_{t1}y_{t2}] = \gamma_{t1t2}exp\left(j(\varphi_{t1} - \varphi_{t2})\right) \qquad (4)$$
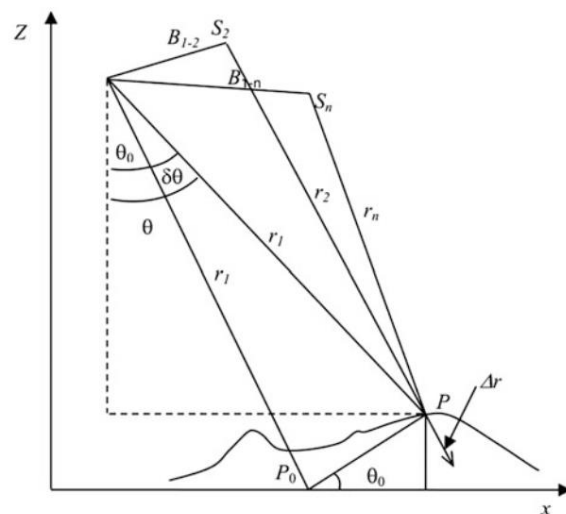
Figure 3. InSAR at point P with N times (Tran et al., 2021a)

In which: y_{t1}- a pixel in the $t1$ SAR image at the considered slant range–azimuth position, y_{t2}- a pixel in the $t2$ SAR image at the considered slant range–azimuth location, γ_{t1t2} - the coherence of the $t1t2$ interferometric pair.

The images should be normalized, thus $E[|y_n|^2] = 1 \forall n$, and the interferometric phases may be written as vectors as follows:

$$\varphi = \psi(\theta) + \alpha \qquad (5)$$

In which: $\varphi = [\varphi_0 \cdots \varphi_{N-1}]^T$ - the vector of the interferometric phases, θ - the vector of the unknown parameters that describe the LDF and residual topography to be estimated, $\alpha = [\alpha_0 \cdots \alpha_{N-1}]^T$ - the atmospheric field or APS, which affects the N acquisitions, and and $\psi(\theta) = [\psi_0(\theta) \cdots \psi_{N-1}(\theta)]^T$ - a vector of known functions of θ.

Multiple image acquisitions with repetition intervals greater than one day can be described using a random process, spatially correlated, and not spatially correlated APS (Tebaldini and Guarnieri, 2010). APS is described as a normal and zero-mean stochastic process with variance σ_α^2 in this case:

$$\alpha \sim N(0, R_\alpha); \ R_\alpha = \alpha_\alpha^2 I_n \qquad (6)$$

In which: I_n - the $N \times N$ identity matrix. Tebaldini and Guarnieri (2010) has a comprehensive description of APS.

Zebker and Villasenor (1992) introduced the set of coherence, γ_{t1t2}, of each pair of the interferogram, which specifies the correlation and lost correlation of the pixels due to various factors such as surface, volumetric, and temporal, in Eq. (7) below:

$$\gamma_{t1t2} = \gamma_0 \gamma_{t1t2}^{sup} \gamma_{t1t2}^{vol} \gamma_{t1t2}^{temp} \qquad (7)$$

We can derive the following equation from Eq. (4) as following:

$$R^{def} = E[yy^H] = \phi \Gamma \phi^H \qquad (8)$$

In which: R - the data covariance matrix; $y = [y_0 \cdots y_{N-1}]^T$ - the stack of SLC images in the slant range, azimuth plane, at a given point (r, x); Γ represents an $N \times N$ symmetric matrix, whose elements are given by the interferometric coherences $[\Gamma]_{t1t2} = \gamma_{t1t2}$; and ϕ - a $N \times N$ diagonal matrix, whose elements are given by the interferometric phases:

$$\phi = diag\{\exp(j\varphi_0) \cdots \exp(j\varphi_{N-1})\} \qquad (9)$$

Our purpose is to extract the deformation phase from the general phases using the PSInSAR approach. The separation of these phases involves the employment of a precise DEM and the identification of permanent scattering points based on the high scattering points found above all image pairs. The processing approach is given in Figure 4. In this article, we used the SNAP toolbox, StaMPS software implementation process for detecting subsidence at PS points (Hooper et al., 2012).

Before importing data into StaMPS, a preparatory step is required. This step relates to the selection of permanent scattering points (PSs) in time series images. The PSs point threshold is dependent on the amplitude dispersion D_A represented as:

$$D_A = \frac{\partial_A}{m_A} \qquad (10)$$

Where: ∂_A - the standard deviation and m_A - the mean of the backscattering intensity. The D_A - the value representing each pixel remains constant in the entire of time series images. Therefore, the amplitude dispersion is an
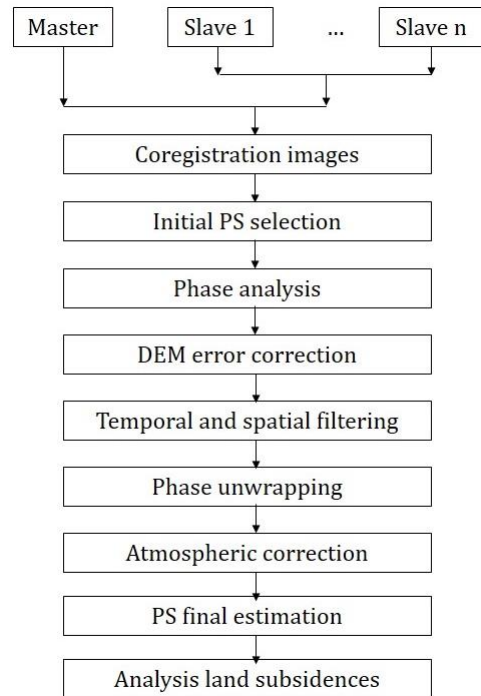
Figure 4. The workflow of PSInSAR processing.

indicator of the stability of a pixel. The smaller the D_A value, the better the pixel stability (Tran et al., 2021a). The default D_A value is usually chosen of 0.4.

4. Results and discussion

StaMPS software was used to process a time series of Sentinel-1A images and determine land subsidence values at PS points with a master image date of March 4th, 2020. Figure 5 shows the displacement velocity along LOS (MLV), which ranges from -23.2 mm to +21.0 mm per year after removing the effect of terrain. However, the land subsidence rate in the study area is not equal (Figure 5). As a result, we assess land subsidence in different areas, including Phan Me coal mine (A), Thai Nguyen city (B), and Trai Cau iron mine (C).

The area surrounding the Phan Me coal mine has been assessed as having significant land subsidence (Figure 5). Currently, the Phan Me coal mine must complete the mining licensing procedure. On March 24th, 2020, at disposal site

No. 3 of the Phan Me coal mine, there were landslides and land subsidences measuring between 4 and 6 centimeters (Trang, 2020). In this article, the applications StaMPS and StaMPS-Visualizer are used to detect land subsidence at PS points over time and estimate the trend of surface displacement. The results of the investigation at the PS points indicate that the Phan Me coal mine has subsidence points above 40 mm (Figure 6b). Additionally, the nearby areas tend to decline (Figure 6c).

Thai Nguyen City has land subsidence ranging between -25 mm and +10 mm (Figure 7a). However, the overall trend of Thai Nguyen City's sites is stable (Figure 7c). At PS points, Thai Nguyen City estimated land subsidence of about 60 mm between 09/2020 and 11/2020 (Figure 7b). Several districts of Thai Nguyen province were reported to be subsiding in August 2020 and November 2020, including Ba Son coal mine in Phu Luong district (Vu, 2020), Pho Yen town in Dinh Hoa district (Cuong, 2020), and Minh Tien coal mine in Dai Tu district (Binh, 2020).
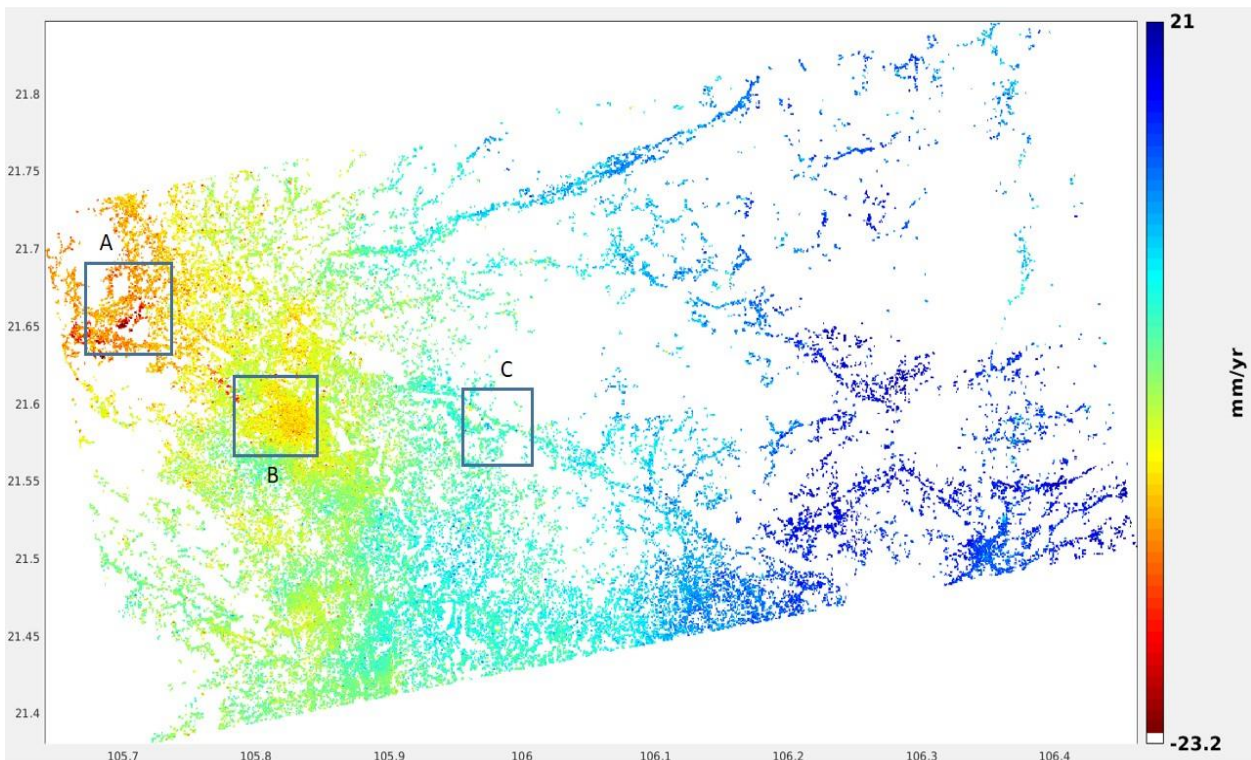
Figure 5. The mean subsidence velocity along LOS (MLV) in -23.2 mm to +21.0 mm/yr; (A) Phan Me Coal Mine; (B) Thai Nguyen city; (C) Trai Cau iron mine.
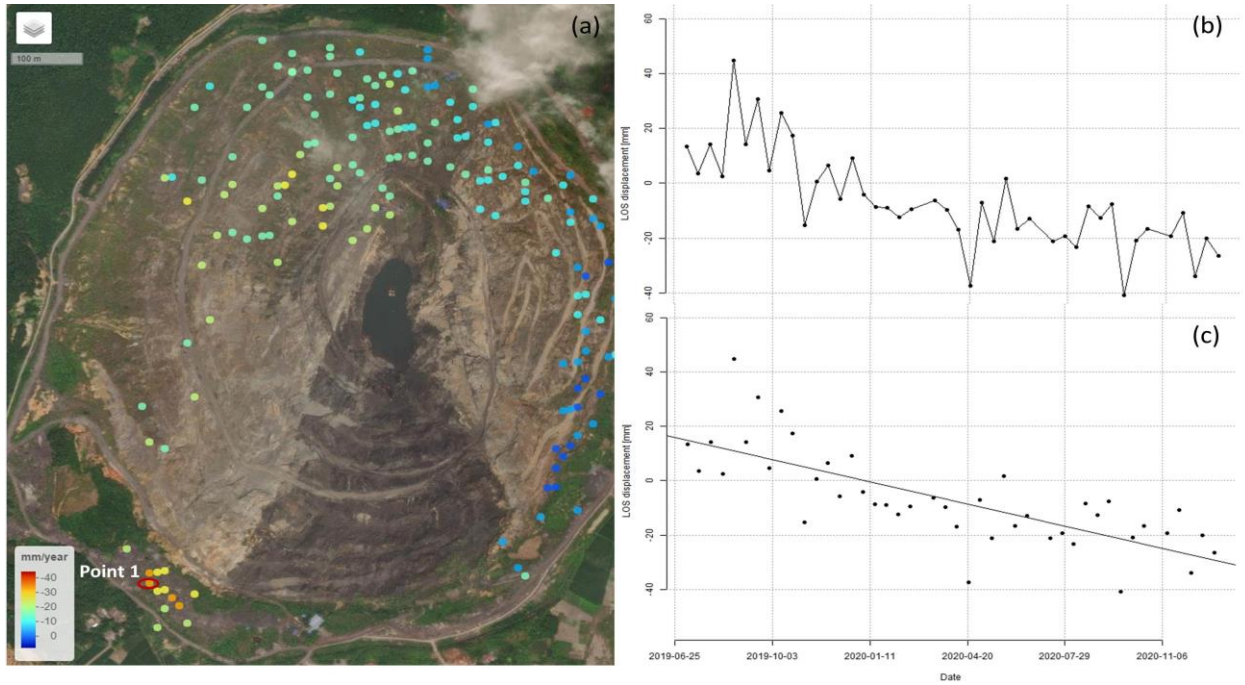
Figure 6. Detection land subsidence at PS points in Phan Me coal mine.
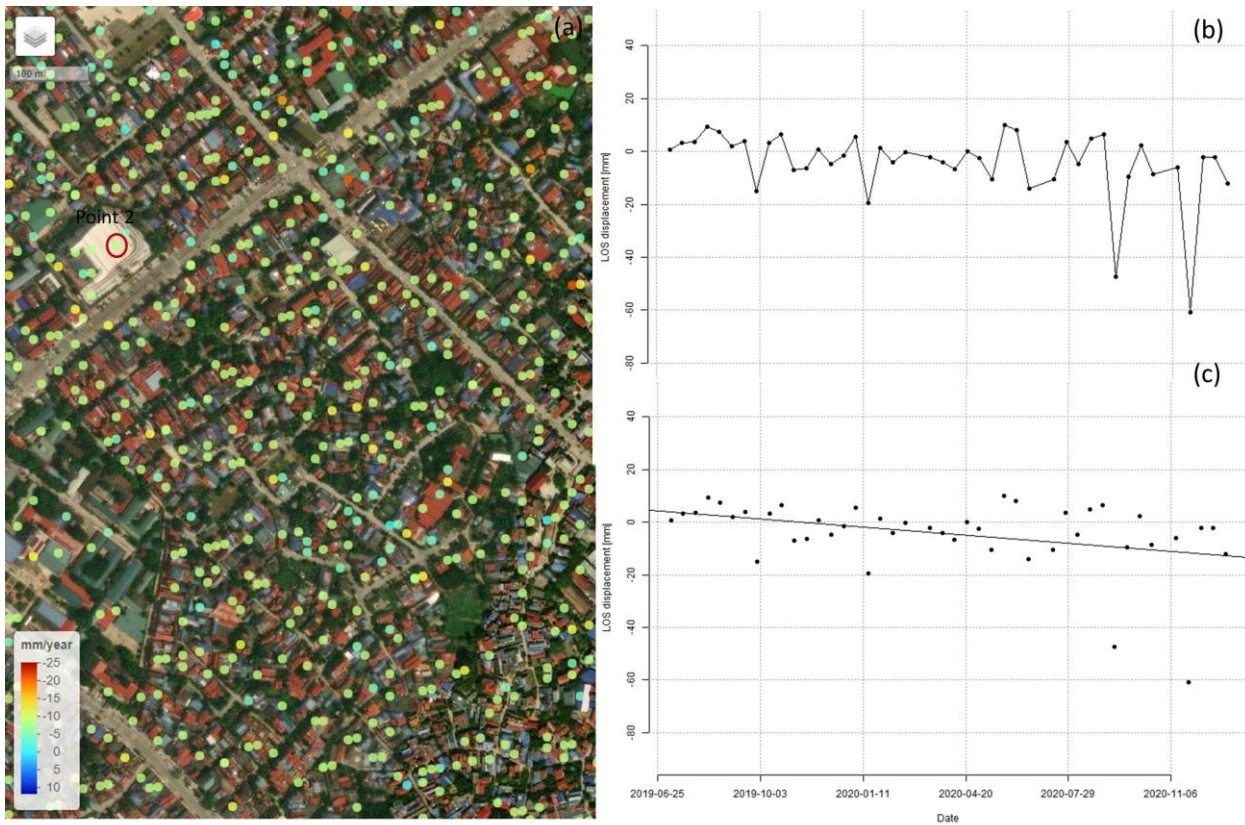
Figure 7. Detection land subsidence at PS points in Thai Nguyen city.
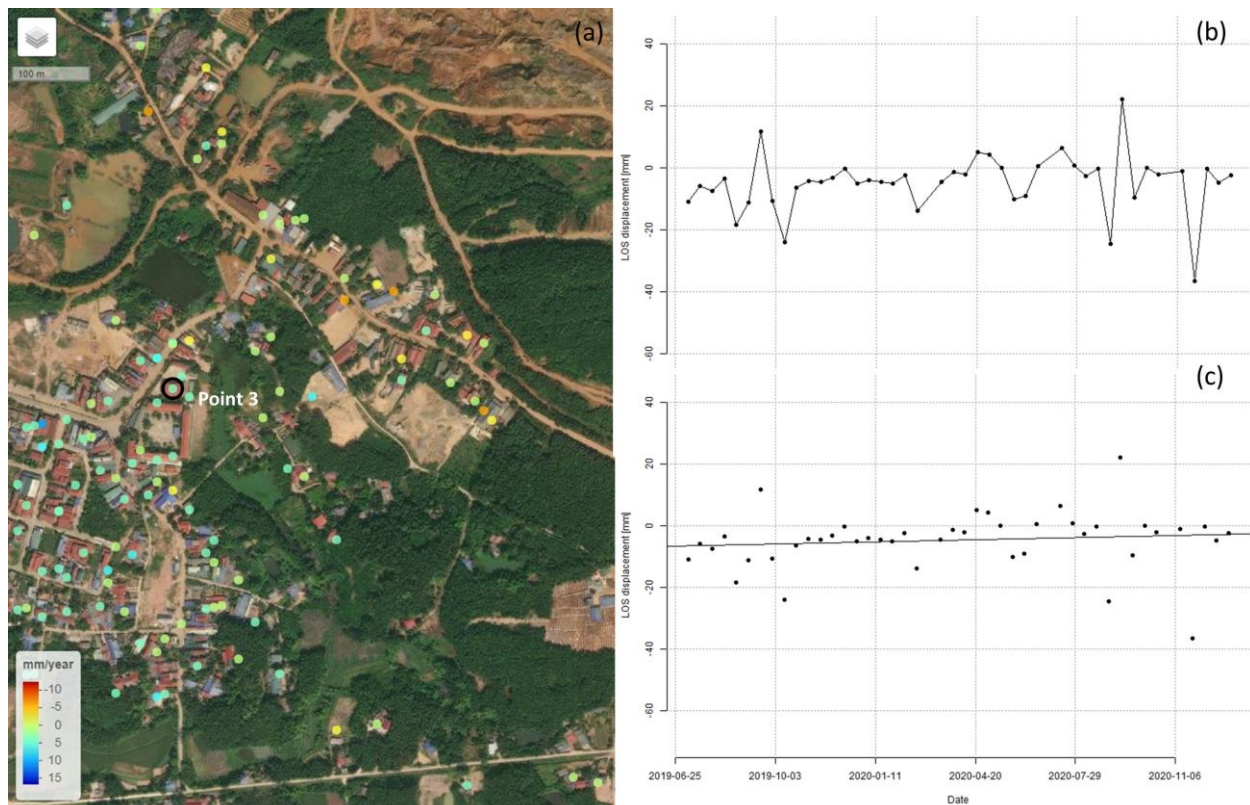
Figure 8. Detection land subsidence at PS points in Trai Cau iron mine.

In 2020, the Trai Cau Iron Mine had a natural trend toward minimal change and was mainly stable. The Trai Cau Iron Mine must close in May 2020 due to the impact of mining activities on the subsidence of nearby structures. (Binh, 2021; Giang, 2020). Similar to Thai Nguyen City, the Trai Cau mine reported an unusual -40 mm land subsidence in November 2020 (Figure 8b). Based on the reports, around 200 abnormal landslides have been observed in the area of the Trai Cau Iron Mine (Binh, 2021). The holes are the result of the dry removal of the deep iron ore layer at Nui Quang, which resulted in the change of the caster geological layers, groundwater loss, and subsidence.

According to that, there was a high correlation between PS totals and urban and barren areas, which have high coherence values. The PS analysis points are placed near permanent buildings, which makes them more accurate than points on soft soils. In mountainous terrain, PS points are largely neglected.

5. Conclusion

In conclusion, the PSInSAR technique is the key tool to estimate surface displacements over a wide range. According to this, the mean displacement velocity in the study area is between -23.2 mm and +21.0 mm per year. In addition, an analysis of land subsidence based on a time series of Sentinel-1A images indicated that this area's surface displacement trends had changed over time. In particular, it shows unexpected movements at certain observation times. According to the analysis results in Thai Nguyen province, the mining activities of coal mines, iron mines, and the exploitation of natural resources have affected the geology of the area, causing geological phenomena. Therefore, the PSInSAR method is used to analyze large-scale surface displacement and makes it easier to monitor the earth's surface using time series Sentinel-1 images, particularly in regions where land subsidence is frequent, such as the Vietnamese province of Thai Nguyen.

Acknowledgments

Satellite data are supported by the European Space Agency (ESA).

Contribution of authors

Hang Minh Le reviewed and wrote the introduction, results and discussion; Anh Van Tran collected documents, data and wrote the methodology and conclusions

References

Balbarani, S., Euillades, P. A., Euillades, L. D.,Casu, F., & Riveros, N. C. (2013). Atmospheric corrections in interferometric synthetic aperture radar surface deformation—A case study of the city of Mendoza, Argentina. *Adv. Geosci., 35*, 105–113.

Bamler, R., & Hartl, P. (1998). Synthetic aperture radar interferometry. *Inverse problems*, *14*, R1

Bateson, L., Cigna, F., Boon, D., & Sowter, A. (2015). The application of the Intermittent SBAS (ISBAS) InSAR method to the South Wales Coalfield, UK. *International Journal of Applied Earth Observation and Geoinformation, 34,* 249-257.

Binh, T. (2020). Coal mining companies must be punished for harming people's lives. *Nhan dan Journal.* https://nhandan.vn/can-xu-nghiem-cong-ty-khai-thac-than-gay-anh-huong-doi-song-nguoi-dan-post625351.html.

Binh, T. (2021). Early to support people affected by subsidence in Trai Cau town. *Nhan Dan Journal.* https://nhandan.vn/tin-tuc-xa-hoi/som-ho-tro-nguoi-dan-bi-anh-huong-sut-lun-o-thi-tran-trai-cau-667077/

Chen, D., Lu, Y., & Jia, D. (2018a). Land deformation associated with exploitation of groundwater in Changzhou City measured by COSMO-SkyMed and Sentinel-1A SAR data. *Open Geosciences*, *10,* 678-687.

Chen, G., Zhang, Y., Zeng, R., Yang, Z., Chen, X., Zhao, F., & Meng, X. (2018b). Detection of Land Subsidence Associated with Land Creation and Rapid Urbanization in the Chinese Loess Plateau Using Time Series InSAR: A Case Study

of Lanzhou New District. *Remote Sensing*, *10*(2), 270.

Conacher, A.J., & Conacher, J. (1995). *Rural land degradation in Australia*. Oxford University Press. Oxford, 192 pages.

Cuong, H. (2020). Need the agreement of the people. *Thai Nguyen News Journal.* https://baothainguyen.vn/tin-tuc/xa-hoi/can-su-dong-thuan-tu-phia-nguoi-dan-276939-85.html.

Dan, T. (2018). Thai Nguyen: Announced the cause of land subsidence. *Natural Resources and Environment Journal.* https://baotainguyenmoitruong.vn/thai-nguyen-cong-bo-nguyen-nhan-sut-lun-dat-nguoi-mung-ke-lo-268324.html

Dang, V. K., Doubre, C., Weber, C., Gourmelen, N., & Masson, F. (2014). Recent land subsidence caused by the rapid urban development in the Hanoi region (Vietnam) using ALOS InSAR data. *Natural Hazards and Earth System Sciences, 14,* 657-674.

Delacourt, C., Briole, P., & Achache, A. J. (1998). Tropospheric corrections of SAR interferograms with strong topography. *Application to Etna. J. Geophys. Res. Lett., 25,* 2849–2852.

Deng, J., Li, T., & Feng, D. (2019). Urban Ground Surface Subsidence Monitoring Based on Time Series InSAR Technology. *IOP Conference Series: Earth and Environmental Science, 283,* 13-14, Nanchang, China, 1-6.

Emardson, T. R., Simons, M., & Webb, F. H. (2003). Neutral atmospheric delay in interferometric synthetic aperture radar applications: Statistical description and mitigation. *Journal of Geophysical Research: Solid Earth*, *108* (B5), 1-8.

Ferretti, A., Andrea, M-G., Prati, C., Rocca, F., & Massonnet, D. (2007). *InSAR Principles: Guidelines for SAR Interferometry Processing and Interpretation.* ESA Publications, The Netherlands, 250 pages.

Ferretti, A., Prati, C., & Rocca, F. (2001). Permanent Scatterers in SAR Interferometry.

IEEE Transactions on Geoscience and Remote Sensing, 39(1), 8-20.

Giang, T. (2020). New sinkhole appeared in Trai Cau town. *Web portal Dong Hy district, Thai Nguyen province.* https://donghy.thainguyen.gov.vn/tin-moi/-/asset_publisher/Pd5HkZs9ZQIG/content/xuat-hien-ho-sut-moi-tai-thi-tran-trai-cau?inheritRedirect=false.

He, Y., Wang, W., Yan, H., Zhang, L., Chen, Y., & Yang, S. (2020). Characteristics of Surface Deformation in Lanzhou with Sentinel-1A TOPS. *Geosciences, 10*(3), 99, 1-21.

Hooper, A., Bekaert, D., Spaans, K., & Arikan, M. (2012). Recent advances in SAR interferometry time series analysis for measuring crustal deformation. *Tectonophysics, 514-517*, 1-13.

Nam, B. X., Tran, V. A., Bui, L. K., Long, N. Q., Le, T. T. H., & Goyal, R. (2021). Mining-Induced Land Subsidence Detection by Persistent Scatterer InSAR and Sentinel-1: Application to Phugiao Quarries, Vietnam. *Proceedings of the International Conference on Innovations for Sustainable and Responsible Mining*, Springer, 108, 18-38.

Pepe, A., & Calo, F. (2017). A Review of Interferometric Synthetic Aperture RADAR (InSAR) Multi-Track Approaches for the Retrieval of Earth's Surface Displacements. *Applied Sciences, 7*(12), 1264, 1-39.

Sandwell, D. T., Myer, D., Mellors, R., Shimada, M., Brooks, B., & Foster, J. (2008). Accuracy and Resolution of ALOS Interferometry: Vector DeformationMaps of the Father's Day Intrusion at Kilauea. *IEEE Transactions on Geoscience and Remote sensing*, *46*(11), 3524-3534.

Tebaldini, S., & Guarnieri, A. M. (2010). Methods and performances for multi-pass SAR interferometry. *Geoscience and Remote Sensing New Achievements.* IntechOpen. 329-356.

Tran, V. A., Masumoto, S., Raghavan, V., & Shiono, K. (2007). Spatial distribution of subsidence in Hanoi detected by JERS-1 SAR interferometry. *Geoinformatics*, *18*(1), 3-13.

Tran, V. A., Tran, Q. C., Nguyen, D. A., Ho, T. M. D., Tran, T. A., Nguyen, N. H., & Luong, T. T. L. (2016). Application of PSInSAR method for determining of land subsidence in Hanoi city by Cosmo-Skymed imagery. *GIS-IDEAS 2016*, 1-9.

Tran, V. A., Bui, X. N., Nguyen, Q. L., & Tran, T. A. (2020). Land Subsidence Detection in Tan My-Thuong Tan Open Pit Mine and Surrounding Areas by Time Series of Sentinel-1 Images. *Inżynieria Mineralna*, *1*(2). 171-180. https://doi.org/10.29227/IM-2020-02-22

Tran, V. A., Tran, Q. C., Nguyen, D. A., Ho, T. M. D, Hoang, A. T., Ha, T. K., & Bui, D. T. (2021a). *Subsidence Assessment of Building Blocks in Hanoi Urban Area from 2011 to 2014 Using TerraSAR-X and COSMO-SkyMed Images and PSInSAR,* Remote Sensing and GIScience, Springer, Switzerland, 127-150.

Tran, V. A., Truong, X. Q., Nguyen, D. A., Longoni, L., & Yordanov, V. (2021b). Landslides Monitoring with Time Series of SENTINEL-1 Imagery in Yen Bai Province-Vietnam. *International Society for Photogrammetry and Remote sensing, 46*(4,) 197-203

Trang, Q. (2020). Thai Nguyen: Unusual landslide occurred at the landfill of Phan Me Coal Mine. *Vietnam News Agency Journal.* https://vnanet.vn/vi/tin-anh/tin-thoi-su-trong-nuoc-1/thai-nguyen-xuat-hien-sat-truot-bat-thuong-tai-bai-do-thai-mo-than-phan-me-4548107.html?img=4547728.

Vu, X. (2020). Thai Nguyen: The risks of mining at the Ba Son coal mine. *Tai nguyen & Moi truong Journal.* https://baotainguyenmoitruong.vn/thai-nguyen-hiem-hoa-khai-thac-mo-than-ba-son-302978.html.

Zebker, H. A., & Villasenor, J. (1992). Decorrelation in interferometric radar echoes. *IEEE Transactions on Geoscience and Remote Sensing*, *30*(5), 950-959.

Zhang, Y., Liu, Y., Jin, M., Jing, Y., Liu, Y., Liu, Y., Sun, W., Wei, J., & Chen, Y. (2019). Monitoring Land Subsidence in Wuhan City (China) using the SBAS-InSAR Method with Radarsat-2 Imagery Data. *Sensors, 19*(3), 743, 1-16.